A&A 478, L23–L26 (2008)
DOI: 10.1051/0004-6361:20078539

Astronomy & Astrophysics

LETTER TO THE EDITOR

The dark matter halo of NGC 1399 – CDM or MOND?⋆,⋆⋆

T. Richtler[1], Y. Schuberth[1,2], M. Hilker[3], B. Dirsch[1], L. Bassino[4], and A. J. Romanowsky[1,5]

[1] Departamento de Física, Casilla 160-C, Universidad de Concepción, Concepción, Chile
e-mail: tom@mobydick.cfm.udec.cl
[2] Argelander Institut für Astronomie, Auf dem Hügel 71, 53121 Bonn, Germany
[3] European Southern Observatory, Karl-Schwarzschildstr.2, Garching, Germany
[4] Facultad de Ciencias Astronómicas y Geofísicas, Universidad Nacional de La Plata, Paseo del Bosque S/N, 1900-La Plata, Argentina; IALP-CONICET
[5] UCO/Lick Observatory, University of Santa Cruz, California, 95064, USA

Received 23 August 2007 / Accepted 14 November 2007

ABSTRACT

Context. Central galaxies in galaxy clusters may be key discriminants in the competition between the cold dark matter (CDM) paradigm and modified Newtonian dynamics (MOND).
Aims. We investigate the dark halo of NGC 1399, the central galaxy of the Fornax cluster, out to a galactocentric distance of 80 kpc.
Methods. The data base consists of 656 radial velocities of globular clusters obtained with MXU/VLT and GMOS/Gemini, which is the largest sample so far for any galaxy. We performed a Jeans analysis for a non-rotating isotropic model.
Results. An NFW halo with the parameters $r_s = 50$ kpc and $\varrho_s = 0.0065\ M_\odot/\mathrm{pc}^3$ provides a good description of our data, fitting well to the X-ray mass. More massive halos are also permitted that agree with the mass of the Fornax cluster as derived from galaxy velocities. We compare this halo with the expected MOND models under isotropy and find that additional dark matter on the order of the stellar mass is needed to get agreement. A fully radial infinite globular cluster system would be needed to change this conclusion.
Conclusions. Regarding CDM, we cannot draw firm conclusions. To really constrain a cluster wide halo, more data covering a larger radius are necessary. The MOND result appears as a small-scale variant of the finding that MOND in galaxy clusters still needs dark matter.

Key words. galaxies: elliptical and lenticular, cD – galaxies: kinematics and dynamics – galaxies: individual: NGC 1399

1. Introduction

The dark matter halos of early-type galaxies are investigated less well than those of spiral galaxies (for a recent review, see Romanowsky 2006). Globular clusters (GCs) and planetary nebulae are the main stellar dynamical tracers, while X-rays can be used at even larger galactocentric distances for a gas dynamical approach. The reliability of a deduced mass profile depends strongly on the number of dynamical probes available. Regarding GCs, it is therefore natural that the rich GC systems of bright elliptical galaxies have so far been the preferred targets for such studies, for example M 87 (Côté et al. 2001), NGC 4472 (Côté et al. 2003), and NGC 4636 (Schuberth et al. 2006). The largest sample until today has been measured for NGC 1399, the central galaxy of the Fornax galaxy cluster. Richtler et al. (2004, Paper I) analyzed the velocities of about 450 GCs out to a galactocentric distance of 40 kpc and found an approximately constant velocity dispersion. The corresponding dark matter halo was found to be consistent with an NFW-halo (see Sect. 5 for the numerical values). The relatively poor knowledge that we have until now regarding the dark halos of early-type galaxies, does not indicate a common behavior such as the constant rotation curves found in spiral galaxies. While the inferred circular velocities of NGC 1399 or NGC 4636 appear to be flat, they seem to rise for M 87, and most strikingly so for NGC 6166 (Kelson et al. 2002), the central galaxy in Abell 2199. In elliptical galaxies of lower luminosity, the projected velocity dispersion can even be falling (Romanowsky et al. 2003), perhaps including the circular velocity. One may speculate that these relate to the environment. The dark halos of central galaxies might be determined by the dark halos of their host galaxy clusters rather than being halos belonging to individual galaxies. However, a larger sample of well-studied galaxies is necessary to arrive at firm conclusions.

We have now augmented the number of GC velocities around NGC 1399 to nearly 660 reaching a galactocentric distance of 80 kpc, which is an unprecedently large and extended sample. In this Letter, we present the implications of this sample for the dark halo, updating the conclusions of Paper I. Moreover, we discuss the dark halo in the context of Modified Newtonian Dynamics (MOND) (e.g. Milgrom 1983; Sanders & McGaugh 2002). The detailed description of the observations, the reduction, and the analysis will be presented in a forthcoming paper (Schuberth et al., in prep.), taking into account the population substructure of the GC system as well as more anisotropic models.

In the following, we adopt a distance of 19 Mpc for NGC 1399.

⋆ Based on observations made with ESO Telescopes at the Paranal Observatories under program ID 70.B-0174.
⋆⋆ Based on observations obtained at the Gemini Observatory, which is operated by the Association of Universities for Research in Astronomy, Inc., under a cooperative agreement with the NSF on behalf of the Gemini partnership: the National Science Foundation (United States), the Particle Physics and Astronomy Research Council (UK), the National Research Council (Canada), CONICYT (Chile), the 5Australian Research Council (Australia), CNPq (Brazil) and CONICET (Argentina).

Article published by EDP Sciences and available at http://www.aanda.org or http://dx.doi.org/10.1051/0004-6361:20078539

2. Observations

Our new data were obtained with the multi-object-spectrographs FORS2/MXU and GMOS at the VLT and Gemini-South observatories, respectively. The GC candidates were selected from the wide-field photometry by Dirsch et al. (2003). The spectroscopic observations of ten MXU masks in seven fields were carried out in visitor mode during three nights (1–3 December 2002) at the European Southern Observatory Very Large Telescope (VLT) facility on Cerro Paranal, Chile. The observations with the Gemini Multi-Object Spectrograph (GMOS) on Gemini-South were carried out in queue mode in November 2003 and December 2004. A total of ten spectroscopic masks in five fields were observed. We then merged the velocity catalogues with the previous velocities of Paper I after having revised the old spectra by cross correlation methods with the same templates used for the new data. The final velocity database comprises 656 GCs; 160 new targets come from FORS2 and 73 targets from GMOS-S. A typical velocity uncertainty is 50 $\mathrm{km\,s^{-1}}$, while it can be considerably higher for the faintest targets, which have a brightness of about $m_R \approx 22.8$.

3. Velocity dispersions

Converting measured velocities to velocity dispersion is not straightforward. Fluctuations may arise from inhomogeneous sampling or from small numbers of outliers (stemming e.g. from erroneous velocities or contaminants belonging to other galaxies – in our case NGC 1404, which is at a projected distance of 54 kpc). Therefore we define a "safe" subsample, where the objects have distances greater than 3 arcmin to NGC 1404, velocity uncertainties smaller than 75 $\mathrm{km\,s^{-1}}$, and magnitudes in the range $21 < m_R < 22.35$. We calculate dispersions by applying the maximum likelihood estimator of Pryor & Meylan (1993), with the individual velocity uncertainties as weights. For the full sample, the dispersion was calculated by moving bins, each bin containing 60 objects with a step of one object. For the "safe" sample, we calculate the dispersion in independent bins. The sample velocities and derived dispersions are shown in Fig. 1.

The velocity dispersion is approximately constant out to 80 kpc, thus continuing the trend found in Paper I. The various curves refer to different models, which are explained in the following sections.

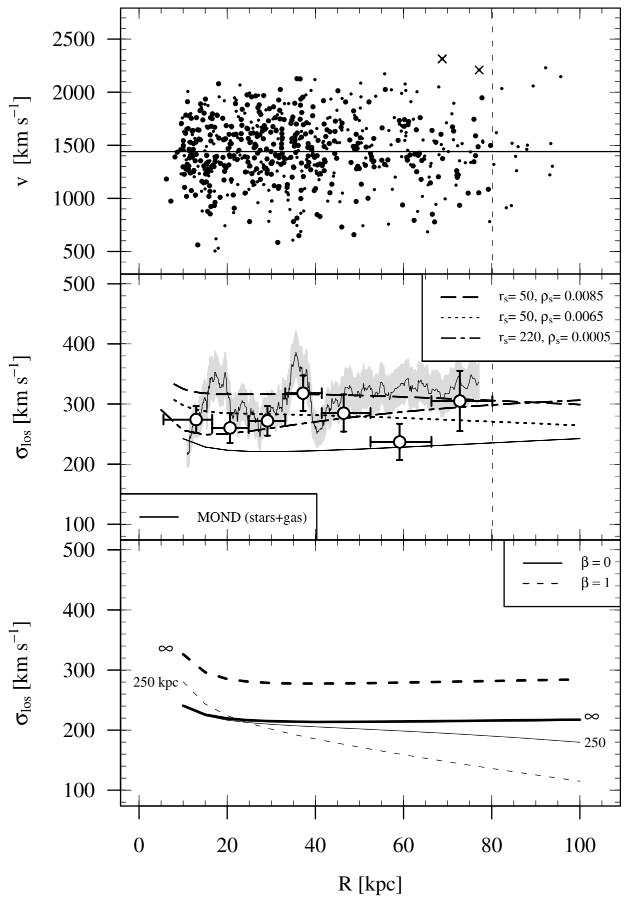

Fig. 1. Kinematics of GCs around NGC 1399. *The upper panel* shows the radial velocities of our total sample versus the radial distance, where 80 kpc correspond to 14.5 arcmin. The two crosses are outlier velocities that we have discarded, and the larger points show objects from the "safe" sample. The horizontal line marks the systemic velocity, and the vertical dashed line indicates the radial limit used for the "safe" sample. *The middle panel* shows the velocity dispersion profile. The thin solid line with shaded region shows the result derived for the full GC sample along with its uncertainties, while the circles with error bars show the "safe" sample. The curves represent various dynamical model fits (isotropic), as described in the text, and with parameters summarized in the legend. The lower solid line represents the expectation from MOND under isotropy. *The lower panel* shows in addition fully radial MOND models (without gas) with a cut-off radius of 250 kpc.

4. Models

In Jeans models that only use velocity dispersions and not higher moments of the velocity distribution, the mass distribution and the orbital anisotropy of the tracer population are degenerate. Here we mainly consider isotropic models, which are good approximations at least to the entirety of those clusters that were found in Paper I to best explain the GC dispersions (see also Côté et al. 2001). In the MOND discussion, we also give fully radial models (which are not realistic) as a guide to how a radial anisotropy affects the results.

We model the projected velocity dispersions under isotropy according to

$$\sigma^2_{\rm los}(R) = \frac{2\,G}{N(R)} \int_R^\infty \frac{\sqrt{r^2 - R^2}}{r^2} \ell(r) M(r) {\rm d}r, \tag{1}$$

where G is the constant of gravitation, $N(R)$ is the projected number density of the tracer population, $\sigma_{\rm los}$ the line-of-sight velocity dispersion to be compared to our observed values, r is the radial distance from the center and R the projected distance, ℓ the spatial (i.e., three-dimensional) density of the GCs, and $M(r)$ the enclosed mass. See e.g., Mamon & Łokas (2005) and van der Marel (1993) for more general analytical solutions of the Jeans equation.

The surface number densities of GCs are adopted from Bassino et al. (2006) as the sum of the number densities for metal-rich and metal-poor clusters, resulting in the 3D density

$$\ell(r) = \frac{N_0}{R_0} \frac{1}{\mathcal{B}\left(\frac{1}{2}, \alpha\right)} \cdot \left(1 + \left(\frac{r}{R_0}\right)^2\right)^{-(\alpha + \frac{1}{2})} \tag{2}$$

with the values $N_0 = 35.54$, $R_0 = 1\overset{\prime}{.}74$, $\alpha = 0.84$, and the Beta-function $\mathcal{B}\left(\frac{1}{2}, \alpha\right) = 2.22$.

As a model for the luminous matter, we adopt the power law given by Dirsch et al. (2003) resulting from the wide-field photometry of NGC 1399 together with a (constant) stellar mass to light ratio, which we fix to $M/L_{\rm R} = 5.5$, following Paper I.

This is about the maximum value, which is found for early-type galaxies (see also Saglia et al. 2000; Bell et al. 2003).

For the shape of the dark halo, we assume an NFW type halo, which for the inner 40 kpc already gave a good description (Paper I). The cumulative mass is

$$M_{\rm dark} = 4\pi \cdot \varrho_{\rm s} \cdot r_{\rm s}^3 \cdot \left(\ln\left(1 + \frac{r}{r_{\rm s}}\right) - \frac{\frac{r}{r_{\rm s}}}{1 + \frac{r}{r_{\rm s}}} \right), \quad (3)$$

where $\varrho_{\rm s}$ and $r_{\rm s}$ are the characteristic density and radius, respectively.

5. Mass profiles

The full sample can be reproduced well by adding an NFW halo with $\varrho_{\rm s} = 0.0085\ M_\odot/{\rm pc}^3$ and $r_{\rm s} = 50$ kpc, the "safe" sample with $\varrho_{\rm s,0} = 0.0065\ M_\odot/{\rm pc}^3$ and $r_{\rm s} = 50$ kpc (long-dashed and dashed line in Fig. 1) to the mass of NGC 1399. As Table 1 shows, the gas mass (which is included in the halo) is negligible within 80 kpc with respect to the stellar mass and unimportant within the virial radius with respect to the dark halo.

The uncertainties are mostly of a systematic nature and difficult to quantify, but these two halos probably embrace the acceptable values with a preference near the "safe" sample in the sense of the best-fit halos.

These halos can now be compared with the X-ray mass profile presented by Paolillo et al. (2002). Figure 2 shows the total mass for the various models; i.e. the NFW halo includes dark matter, gas, and the stellar matter outside NGC 1399; however, it is vastly dominated by dark matter. The overall agreement of the X-ray mass profile, particularly with the "safe" halo, is very good. There is no support however for the steep rise between 20 and 40 kpc and the subsequent flat part, which would mean a strong decline in the mass density to almost zero. This feature has been already noted in the ASCA study of Ikebe et al. (1996), who interpreted it as the transition radius between the galaxy and the cluster potential. Such a mass profile would probably be dynamically unstable, so we suspect that it is possibly a consequence of azimuthally averaging over a disturbed intensity field. The "safe" halo has a high concentration and only marginally fits to the simulations of Bullock et al. (2001), but better than the halo from Paper I. The virial radius is 670 kpc, the mass inside this radius is $1.8 \times 10^{13}\ M_\odot$, and the concentration $c = 13.4$. Until now, the only dynamical analysis of the Fornax cluster is that of Drinkwater et al. (2001; hereafter DEA), who used galaxy velocities to constrain the cluster mass.

To investigate what one would expect from the DEA mass for the projected velocities in our radial range, we describe the DEA mass by an NFW profile (which includes dark matter and baryons, but not NGC 1399) with the parameters $\varrho_{\rm s,0} = 0.0005\ M_\odot/{\rm pc}^3$ and $r_{\rm s} = 220$ kpc, which reproduces the solid line in Fig. 4 of DEA out to 1 Mpc very well. To compare this model to the GC dispersions in the inner regions of the halo, we add in the stellar mass of NGC 1399, and show the modeling result in Fig. 1. Although this halo model was not among our best fits, it is also not excluded, as it seems to follow the velocity dispersions quite well. However, it falls below the X-ray mass model at small radii (Fig. 2). The difference between the mass profile of DEA and our "safe" halo is listed in Table 1. The gas mass of Paolillo et al. (2002) is also given. It is only known out to about 200 kpc, and thus is extrapolated to larger radii. Table 1 shows that the agreement of our halos with the mass of DEA is unsatisfactory. It becomes even worse at larger radii: at 1 Mpc, the DEA mass is $6 \pm 2 \times 10^{13}\ M_\odot$ versus our mass of $2.2 \times 10^{13}\ M_\odot$ ($2.9 \times 10^{13}\ M_\odot$ for the more massive halo). We conclude that, although our sample is already the largest one available, we are not able to conclusively distinguish between different halos on a cluster-wide scale. There is, however, evidence from the data of Bergond et al. (2007) that our halo might be extrapolated out to 200 kpc (Schuberth et al. 2008).

Table 1. The table lists the masses of different components or halos for two radii, the larger one being the virial radius of the "safe" halo. All values are given in units of $10^{12}\ M_\odot$. The stellar mass at 670 kpc is an extrapolation of the NGC 1399 luminosity profile and serves as a proxy for the total stellar mass. The gas mass is taken from Paolillo et al. (2002) and is extrapolated beyond 200 kpc. The "safe" halo is explained in the text. "DEA-mass" denotes the Fornax cluster mass according to Drinkwater et al. (2001).

Radius	Stellar mass	Gas mass	"safe" halo	DEA-mass
80 kpc	0.6	0.04	3.5	2.9
670 kpc	1.1	1.5	18	43

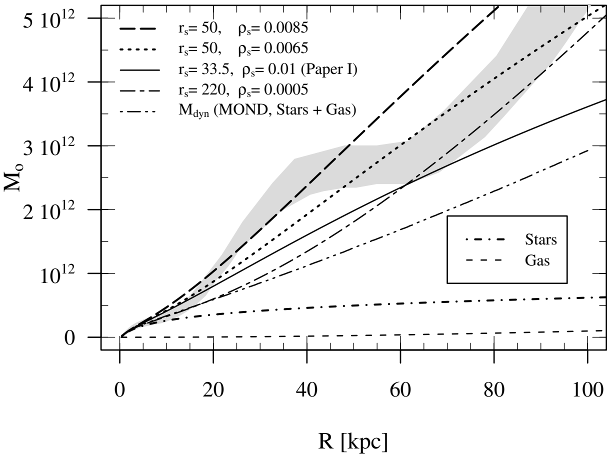

Fig. 2. Comparison to X-ray measurements. The grey area shows the range of the mass models presented by Paolillo et al. (2002). The short-dashed line refers to our preferred halo, the long-dashed line to the halo derived from the full sample. The solid line is the halo derived in Paper I. The stellar mass is shown as dashed-dotted line. The dynamical MOND mass is shown as the dot-dot-dashed line.

6. Modified Newtonian dynamics

As an alternative to the CDM paradigm, Milgrom's MOND (e.g. Milgrom 1983; Sanders & McGaugh 2002) is mostly successful in accounting for the kinematics of disk galaxies and/or the baryonic Tully-Fisher relation (McGaugh 2005). Little is known about early-type galaxies. Schuberth et al. (2006) find that NGC 4636 is indeed consistent with MONDian kinematics. Also the declining velocity dispersion of NGC 3379 (Romanowsky et al. 2003) does not necessarily contradict MOND (Milgrom & Sanders 2003). However, on the scale of galaxy clusters, MOND apparently needs additional dark matter (e.g. Sanders 2003; Pointecouteau & Silk 2005). It is therefore interesting to investigate whether NGC 1399, as a central galaxy, is compatible with MOND or not.

Assuming spherical symmetry, we apply the classic MOND recipe $g_{\rm N} = \mu(g/a_0) \cdot g$, where g and $g_{\rm N}$ are the MOND acceleration and Newtonian acceleration, respectively, a_0 a universal constant, and $\mu(g/a_0)$ is a function interpolating between the Newtonian and the MONDian regimes.

Following Famaey & Binney (2005), we adopt $\mu = x/(1+x)$ with $x = g/a_0$ (see also Zhao & Famaey 2006). The circular velocity curve then reads

$$V^2_{\mathrm{circ},M} = \frac{V^2_{\mathrm{circ,N}}}{2} + \sqrt{\frac{V^4_{\mathrm{circ,N}}}{4} + V^2_{\mathrm{circ},N} \cdot a_0 \cdot r}, \quad (4)$$

where $V_{\mathrm{circ,N}}$ is the Newtonian circular velocity. For a_0 we adopt the value recommended by Famaey et al. (2007): 1.35×10^{-8} cm s^{-2}. The analysis strongly depends on the shape of the interpolation, since g is comparable to a_0 even at 80 kpc. Adopting the Bekenstein (2004) interpolation function would increase V_{circ} significantly, but it does not fit spiral rotation curves.

To calculate the MOND projected velocity dispersion, we used the standard Jeans equation, with the Newtonian mass corresponding to the MONDian circular velocity. The MOND modeling results are shown in Fig. 1. Under isotropy, the MOND dispersions are significantly lower than the profile derived from the GC dynamics.

Fully radial models are shown in the lower panel. We caution that, in contrast to the isotropic case, the outer integration limit now gains importance. Integrating to infinity, the MOND dispersion could reproduce the data. However, we do not have infinitely distant GCs. The extension of the GCS is about 250 kpc (Bassino et al. 2006). The model for cut-offs of 250 kpc shows that a more realistic radial model does not help in achieving better agreement with MOND. We therefore conclude that MOND does not explain the dynamics of NGC 1399 without additional dark matter.

Such an additional hypothetical dark halo must have a relatively small core and a rapidly declining density profile in order to avoid an increasing circular velocity. Without claiming precision, a halo like $\varrho_{\mathrm{add}} = 0.05\, M_\odot/\mathrm{pc}^3 (1 + r/12)^{-4}$, where r is in kpc, would suffice. It corresponds to adding a dark mass of $7 \times 10^{11}\, M_\odot$ within a radius of 80 kpc, comparable to the stellar mass.

The extension of this MOND model to 1 Mpc predicts a circular velocity corresponding to a Newtonian mass of $4.5 \times 10^{13}\, M_\odot$ – which agrees better with the DEA mass. We also caution that the MOND dispersion at a radius of about 200 kpc has not yet been ruled out (Schuberth et al. 2008). Moreover, the amount of gas beyond 200 kpc is not well-constrained. The necessary dark halo does not falsify MOND, but probably reflects the general finding that MOND fails in galaxy clusters without invoking a dark matter component. Sanders (2007) proposes neutrinos; but since even very cold neutrinos are not expected to clump on scales below a few hundred kpc, this would not be a viable hypothesis for NGC 1399. Other possibilities are molecules (but then how avoid star formation?) or warm-hot intergalactic gas (e.g. Takei et al. 2007). Given that only 10% of the baryons at low redshift have been identified (e.g. Bregman 2007), the amount of gas needed is not in imbalance with the missing baryons. It would, however, be surprising to find such an amount of gas. Future observations with increased sensitivity might well potentially falsify this scenario.

7. Conclusions

We have used our new sample of about 660 velocities of GCs to constrain the dark halo of NGC 1399 within 80 kpc. The resulting halo, assumed to be of the NFW type, is more concentrated than the halos from cosmological simulations, but marginally in agreement. A more massive alternative halo, which would account for the total mass of the Fornax cluster as estimated by Drinkwater et al. (2001), may also be consistent with our data. We are thus not able to conclusively constrain the cluster-wide halo from probes within 80 kpc. We also consider the MOND case and find that MOND is not able to reproduce the observed GC kinematics under isotropy without invoking an additional dark matter component, as already found for other galaxy clusters. A realistic radial anisotropy does not change this conclusion. Moreover, only the isotropic model reproduces the X-ray mass well. The hypothetical dark halo must have a small core, and thus neutrinos do not seem to be viable candidates. It may be in gaseous form. Under our assumptions (particularly the interpolation between the MONDian and the Newtonian regime), MOND makes a strong prediction, which perhaps will be falsifiable in the future.

Acknowledgements. We acknowledge helpful discussions with Benoit Famaey and thank an anonymous referee for clarifying comments. This work has been supported by the Chilean Center of Astrophysics Conicyt FONDAP Nr. 15010003 and by the Deutsche Forschungsgemeinschaft (DFG project HI-855/2). A.J.R. was also supported by NSF Grant AST-0507729.

References

Bassino, L. P., Faifer, F. R., Forte, J. C., et al. 2006, A&A, 451, 789
Bekenstein, J. D. 2004, Phys. Rev. D, 70, 083509
Bell, E. F., McIntosh, D. H., Katz, N., & Weinberg, M. D. 2003, ApJS, 149, 289
Bergond G., Athanassoula, E., Leon, S., et al. 2007, A&A 464, L21
Bregman, J. 2007, ARA&A, 75, in press
Bullock, J. S., Kolatt, T. S., Sigad, Y., et al. 2001, MNRAS, 321, 559
Côté, P., McLaughlin, D. E., Hanes, D. A., et al. 2001, ApJ, 559, 828
Côté, P., McLaughlin, D. E., Cohen, J. G., & Blakeslee, J. P. 2003, ApJ, 591, 850
Dirsch, B., Richtler, T., Geisler, D., et al. 2003, AJ, 125, 1908
Drinkwater M. J., Gregg, M. D., & Colless, M. 2001, ApJ, 548, L139
Famaey, B., & Binney, J. 2005, MNRAS, 363, 603
Famaey, B., Gentile, G., Bruneton, J.-Ph., & Zhao, H. S. 2007, Phys. Rev. D, 75, 063002
Ikebe, Y., Ezawa, H., Fukazawa, Y., et al. 1996, Nature, 379, 427
Kelson, D. D., Zabludoff, A. I., Williams, K. A., et al. 2002, ApJ, 576, 720
Mamon, G. A., & Łokas, E. L. 2005, MNRAS, 363, 705
McGaugh, S. S. 2005, ApJ, 632, 859
Milgrom, M. 1983, ApJ, 270, 365
Milgrom, M., & Sanders, R.H. 2003, ApJ, 599, L25
Paolillo, M., Fabbiano, G., Peres, G., & Kim, D.-W. 2002, ApJ, 565, 883
Pointecouteau, E., & Silk, J. 2005, MNRAS, 364, 654
Pryor, C., & Meylan, G. 1993, Structure and Dynamics of Globular Clusters, ASP Conf. Ser., 50, 357
Richtler, T., Dirsh, B., Gebhardt, K., et al. 2004, AJ, 127, 2094 (Paper I)
Romanowsky, A.J., Douglas, N. G., Arnaboldi, M., et al. 2003, Science, 301, 1696
Romanowsky, A. J., 2006, in Globular Clusters – Guides to Galaxies, ed. T. Richtler & S.S. Larsen, ESO Astrophysics Symposia (Springer Verlag), in press [arXiv:astro-ph/0609251]
Saglia, R. P., Kronawitter, A., Gerhard, O., & Bender, R. 2000, AJ, 119, 153
Sanders, R. H. 2003, MNRAS, 342, 901
Sanders, R. H. 2007, MNRAS, submitted [arXiv:astro-ph/0703590]
Sanders, R. H., & McGaugh, S. S. 2002, ARA&A, 40, 263
Schuberth, Y., Richtler, T., Dirsch, B., et al. 2006, A&A, 459, 391
Schuberth, Y., Richtler, T., Bassino, L., et al. 2008, A&A, 477, L9
Takei, J., Henry, J. P., Finoguenov, A., et al. 2007, ApJ, 655, 831
van der Marel, R. P., & Franx, M. 1993, ApJ, 407, 525
Zhao, H. S., & Famaey, B. 2006, ApJ, 638, L9